Design Optimization of Modular Permanent Magnet Machine with Triple Three-Phase for Aircraft Starter Generator

Bo Wang, Antonino Rocca, Gaurang Vakil, Tao Yang, and Chris Gerada
University of Nottingham

Abstract

Permanent magnet (PM) electrical machine has far-reaching impacts in aviation electrification due to the continuous development in high power density and high efficiency electrical drives. The primary barrier to acceptance of permanent magnet machines for safety-critical starter-generator systems is its low fault-tolerance capability and low reliability (for the conventional designs). This article investigates a modular triple three-phase PM starter-generator comprehensively, including the tradeoff of fault-tolerant topology, optimization design process, analysis of electromagnetic (highlight the post-fault analysis) and thermal behavior, respectively. The triple three-phase segmented topology proposed meet the fault-tolerant requirement along with complete electrical, magnetic, and thermal isolation. There would be cost penalty on the proposed topology, but it gets offset by the ease of manufacturing of coils and their insertion. The stator gaps are introduced while doing segmentation which would provide unique opportunity to provide innovative cooling solutions. The multi-objectively optimization method is employed to search an optimal candidate of modular-designed machine. The detailed electromagnetic analysis of this candidate has been performed, while the post-fault performances have been highlighted, especially under the short-circuit scenarios. After that, the thermal behavior of this modular machine has been studied by the means of Computational Fluid Dynamics (CFD). By a parametric analysis, the varied size of segment gap seems no effect to the thermal management. Moreover, the housing water jacket cooling method is chosen to make the machine work safely. In all, this modular-designed triple three-phase machine meet the requirement for an aircraft application with complete fault tolerance and increased reliability.

Introduction

With continuous progressing in high power density and high efficiency faster than ever, permanent magnet synchronous machine (PMSM) has far-reaching effects in aviation electrification. For the concern of reliability, fault tolerance (FT) is a prerequisite for PMSM as a safety-critical application in more electric aircraft. The fundamental FT requirements have been reviewed comprehensively, which key solutions include fault isolation and suppression of fault current[1].

PMSM with fractional slot concentrated winding (FSCW) provides many merits in terms of fault tolerance [2], particularly the single layer (SL) windings which exhibits few mutual coupling between phases as well as physical separation, due to the non-overlapping windings. To improve the electromagnetic performance, some innovative topologies have been attempted. Aimed at modifying space harmonics, a novel 12-slot/14-pole, single layer winding, PM electrical machine has been investigated [3]. Compared with conventional topology, the novel solution validated the improvement in working harmonic and reduction in rotor loss, by magnetic flux barriers in the tooth.

The SL windings provide the possibility to segment the whole stator assembly to small independent components, along the center line of the unwounded stator teeth. A thorough and comprehensive electromagnetic analysis have been done about modular PM machine, which inserting flux gaps into stator teeth [4-6]. The basic electromagnetic characteristics have been investigated based on parametric stator flux gap with varied width. The general conclusions have been concluded regardless the slot/pole combinations, which highlight the benefit in decreasing the mutual inductance. The analytical expressions of modular machine with absence of stator yoke have been deduced [7]. The analysis paved the way to select proper slot/pole combination which could get balanced candidates between pros and cons, manufacturing benefit and electromagnetic loss, respectively.

Based on the philosophy of fault isolation and maintaining operation, multiple three-phase topology has been an important solution to meet the FT requirements of the applications in transportation electrification [8-13], especially for the safety-critical application. The independent winding sets, or stator sectors, provide the redundancy, partitioning and fault isolation in the presence of electrical fault. The feasibility of multiple three-phase topology is depended on slot/pole combination and winding arrangement, which available combinations have been concluded in [14], based on specific criterions.

Besides the fault's isolation, the inherent capacity of machine to inhibit faulty current, especially the turn-to-turn short-circuit, is a direct way to protect remaining parts to maintain output. The high reactance design could suppress the fault current in the presence of short-circuit [15]. The relation between inductance of machine and parameters have been investigated [16]. Meanwhile, the short-circuit current is sensitive to the position of faulty parts [17]. In addition, low-rotor-pole-number machines have a better fault tolerance capability, while high-rotor-pole-number machines are lighter and provide higher efficiency.

It is worthy to investigate the topology of integration of FSCW and multiple three-phase topology, which combine the merits of fault tolerance, applied on more electric aircraft (MEA).

Besides the aggressive electromagnetic design, the effective thermal management is another cornerstone of high power density machines. General approaches for thermal analysis of electrical machines have been and presented [18]. The theoretical and numerical methods have strengths and weaknesses in accuracy, calculation speed/computation time and available resources. Computational Fluid Dynamics, which is a numerical approach based on the FVM method, has been extensively utilized and validated [19-21]. An improved 3D LPTN method, aimed to multisector triple three-phase electrical machine, has been proposed in [22].

To improve the thermal conduction by decreasing the equivalent thermal resistance between the hot spot and the cooling channel, a small extension of back-iron has been proposed [23]. As the machine hot-spot, cooling on its end-windings by pipes, is a direct way to improve thermal management [24]. Comparative study of electrical machine cooling system has been reviewed [25]. To avoid overheating in the high power density electrical machine, the cooling methods could be cooling jacket, stator cooling, rotor cooling or their combinations.

The thermal analysis on multiphase machines has been investigated, whereas it is still difficult to find technical papers reporting the thermal behavior of multisector machines. Based on specific application, the main objectives of this paper are to investigate the electromagnetic and thermal behavior of a modular triple three-phase machine.

The application requirements, limitation and the initial design are presented in Section 2. In section 3, the machine design process and validation are introduced. To investigate the thermal management, several cooling solutions have been carried out in Section 4.

Modular triple three-phase

As aforementioned in Section I, this paper designs a machine topology to meet the requirements of a starter-generator for the aircraft. The fundamental requirements of this machine are fault tolerance and high power density. In this section, the selection of topology and design process will be introduced.

Fault-tolerant topology

The introduction in the previous section has reviewed the current direction to improve the capacity of fault tolerant. Based on these conclusions, the preliminary selection for this machine is single layer fractional slot concentrated winding with multiple three-phase. The feasibility of potential slot/pole combination candidates are determined by electromagnetic in Table 1, including 12/10, 18/12, 36/8 and 26/10. In the TABLE I, the tick ('√') and cross ('×') represent whether this topology is feasible or not, separately. While power electronics involves high costs and high power ratings, the triple three-phase method is a compromise candidate with benefits in cost, redundancy and post-fault performance. Meanwhile, 18/12 combination is better than 36/10 due to higher pole pairs, which related to higher efficiency.

Table 1. Feasible slot/pole combination candidates.

Combination	2×3-phase	3×3-phase	6×3-phase
12/10	√	×	×
18/12	×	√	×
36/8	×	×	√
36/10	√	√	√

Further design has been added to improve the conventional topology to modular one by cutting the whole stator to nine independent segments, shown in Figure 1 (a). The 9 segments are arranged to form three independent three-phase machine (1-2-3, 4-5-6 and 7-8-9), and the phasor diagram of this machine is shown in Figure 1 (b). The triple three-phase topology exhibits the better fault tolerance due to independent electrical circuit and nonoverlapped windings between different three-phases. Furthermore, the segment gaps provide the space to insert another material to improve the thermal conduction.

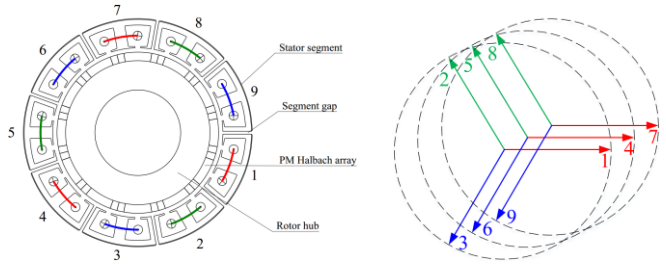

Figure 1. 18 slot/12 pole modular triple three-phase machine (a) Cross section. (b) EMF phasor diagram.

Multiple-objective optimization

Researchers have reached a consensus that electrical machine design is a multiple-objective and multiple discipline-design process rather than electromagnetic issue, especially for high power density of high power machine. To get an optimal candidate, the optimization design process has been adopted, as detailed in [14]. In optimization design, the Motor-CAD® and non-dominated sorting genetic algorithm (NSGA-II) in modeFRONTIER® utilizing the MATLAB® scripts are respectively employed for the analyses and iteration calculations.

Selection of Variables

In the electrical machine design process, considerable dimensions or electrical values are related to the performance, results of electromagnetic, mechanical and thermal. The first priority of the process is to choose appropriate variables, input and output, for the workflow. The selected input variables should sensitive to affect the output performance directly, such as electrical load. The scope of input variables should be assigned reasonably to avoid interference. Meanwhile, the output variables are the criterions during the iterations. The selection of variables for the design process are listed in Table 2.

Table 2. Variables selection for machine optimization

Variables	Selection
Input	diameter of stator bore, width of tooth, depth of slot, opening of slot, depth of tooth tip, angle of tooth tip, thickness of sleeve and thickness of magnet

Constraints and Objectives

Introduced in the abovementioned part, some output variables are criterions or constrains to judge the candidate if it is feasible. These output variables, as constraints, should be assigned specific value critically before the start of the workflow. In this model, the output power (***P***), torque ripple, efficiency (***η***), winding temperature (***Tw***) and line-lint voltage (***U***) are selected as constraints with specific values, respectively. The motor-CAD provide the thermal management results based on LPTN methods, such as the temperature of components. The cooling method will be introduced in following sections.

As an aircraft application, it is a critical objective to pursue high power-density which is a ratio of output power (***P***) over mass (***W***). Subsequently, the fault tolerance is another objective for this application and short-circuit current (I_{sc}). To cope the most severe fault in the electrical machine side, I_{sc}. These three objectives provide the optimization with directions. Above all, output variables selected for the workflow are list in Table 3, with quantitative or qualitative definitions.

Table 3. Variables selection for machine optimization.

Output variables	Constraints	Objectives
Output power, P	>35000 W	Maximize
Weight, W	-	Minimize
Torque ripple	< 5 %	-
Efficiency, □	> 95 %	-
Short-circuit current, Isc	-	Minimize
Winding temperature, TW	< 200 ℃	-
Line-line voltage, U	< 513 V	-

Workflow and Optimization

The workflow of the electrical machine is depicted in Figure. 2 which consists of variables, design of experiment (DOE), multiple-discipline analysis, data process and iterations. Firstly, the initial conditions are created and connected to the design variables. Secondly, the input variables are imported into Matlab and the electromagnetic models and following thermal management calculations are automatically operated to calculate the output variables s by Motor-CAD. Thirdly, every calculated result is evaluated with constraints to select the feasible design and generate new design, which generated by using NSGA-II in modeFRONTIER. These arrows represent the objectives which are expected.

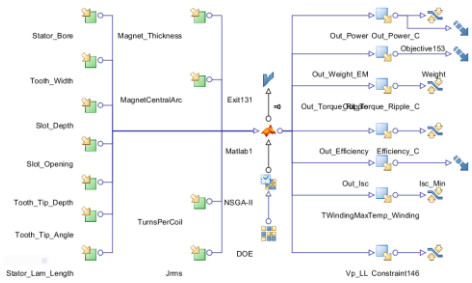

Figure 2. Multiple-objective design workflow in ModeFRONTIER®

Searching Optimal Design

After the comparison with constraints, all the feasible designs could be filtered out. A bubble chart illustrates the visualization of values of weight-power plane with the short-circuit current being shown as bubble color, in Figure 3. The classical method of Pareto front is a general approach for searching optimal design in a two-objective optimization, which is unapplicable for this application.

Afterwards, the multiple criterion decision maker (MCDM) method could be adopted to rank feasible candidates. The multiple-objectives optimization results could be transformed to single objective optimization by assigning weighting factors, which is easier to rank and select. In this model, these objectives are assigned equal weighting factors, 1/3, balancing the requirements of high-power density and fault tolerant.

After the rank, the parameter of optimal design is shown in Table 4, the detailed electromagnetic and thermal management will be shown in following sections.

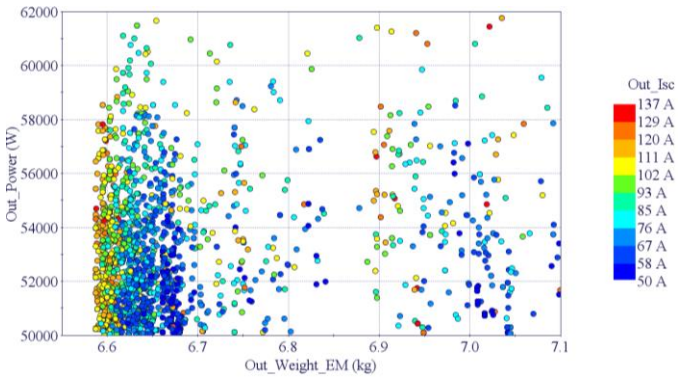

Figure. 3. Bubble chart of three output variables, weight (kg), output power (W) and short-circuit current (A)

Table 4 Parameters of optimal design

Variables	Value	Unit
Stator bore	119	mm
Tooth width	8	mm
Slot depth	16	mm
Slot opening	4	mm
Tooth tip depth	1	mm
Tooth tip angle	0	degree
Magnet thickness	6	mm
Central magnet angle	90	degree

Inductance

The main objective of machine design is to pursue high fault tolerance. The magnetic isolation is key part, accomplished by low mutual inductance between faulty and healthy windings[26, 27]. Under the severe faulty scenarios, especially short-circuit faults, faulty winding could put the healthy winding at risk by induced voltage derived from faulty current.

To illustrate the mutual inductance which between the three set of three-phase windings (1-2-3, 4-5-6 and 7-8-9), there is a quantitative ratio which determined by maximum mutual inductance (M) over minimum self-inductance (L) in triple three-phase inductance matrix. Based on the optimal design, the inductances values could be got from FEM results. The 3D stem plot of self-inductance and mutual inductance are illustrated in Figure. 4. Compared with self-inductance, in the position of diagonal, the mutual inductance is too low to affect magnetic flux in adjacent windings, which is expected for a fault tolerant machine.

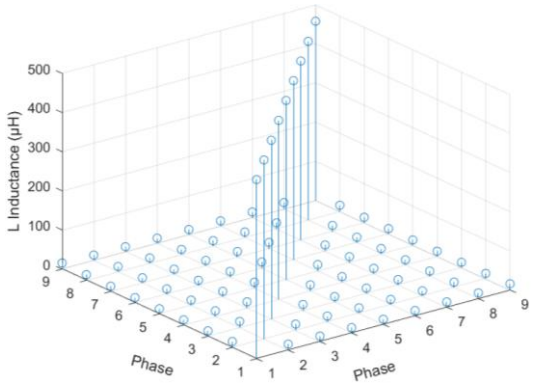

Figure. 4. Matrix diagram of self-inductance and mutual inductance

Design validation

In this section, a detailed finite element analysis (FEA) for the optimal triple three-phase machine will be given to illustrate the comprehensive performance, especially under the faulty scenarios. The machine dimensions are based on the optimal design variables.

To compare the performance between healthy and faulty operations, the whole machine model is created. The FEA results, including the open-circuit, on-load operation and short-circuit operation, will be illustrated, respectively.

Open-circuit

Due to topology design, the spatial results of three three-phases are totally same and overlapped, including but not limited to linkage, back EMF or current. Consequently, the results will focus on one three-phase section, such as first section.

Flux linkage

The flux linkage distribution of modular triple three-phase machine under the open-circuit is shown in Figure. 5(a), compared with conventional topology, as shown in Figure. 5(b). The flux density in airgap is shown in Figure. 6, while the position of poles and stator tooth aligned in the direction which represented the maximum linkage of Phase 1. Due to the modular design and segment gaps, the flux path has been changed significantly between the adjacent phases.

The demerits of this sort of design have been validated that the presence of segment gaps could make the cogging torque magnitude higher because of more flux leakage through the tooth tips [6]. Moreover, the unequal slot-opening width and segment gaps can cause affect the cogging torque in peak value and periodicity. Oppositely, the segment gaps make it more difficult for some of flux to get into adjacent phases, because the reluctance of gap is significant high than stator. The existence of segment gaps influences the flux distribution, which benefits the magnetic isolation of phases. Meanwhile, the thermal dissipation path is changed as well.

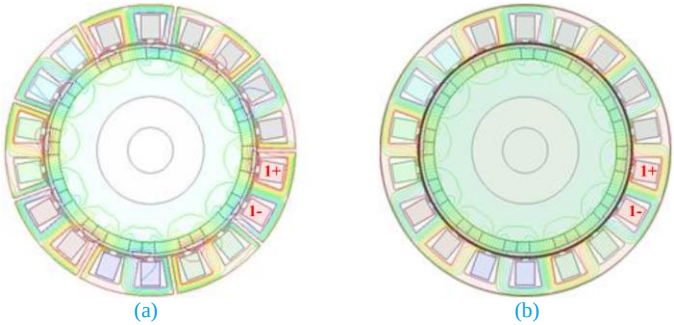

(a) (b)

Figure 5. Flux plot distributions under open-circuit in the machine components (a) Modular segments. (b) Conventional topology.

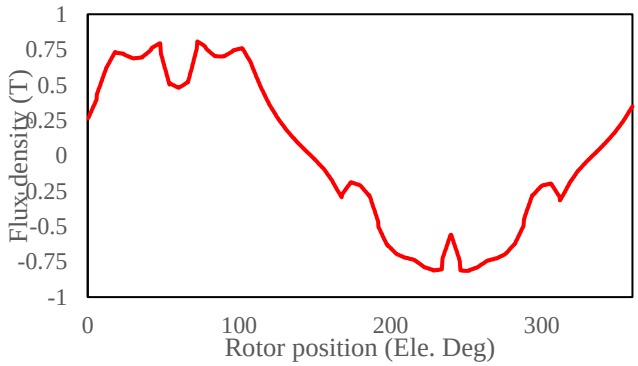

Figure 6. Air-gap flux density versus rotor position.

Back-EMF

The induced voltage, phase back EMF of PMSM is determined by the airgap flux density and winding factor. The phase back EMF could be calculated by the product of rotational speed, fundamental winding factor, number of turns, diameter of airgap, and the length of lamination stack. In the conventional topology, winding factor, comprising of winding distribution factor and coil pitch factor, could be calculated by general theoretical equations. And, the winding factor for 18 slot/12 pole is 0.866. For this case, triple three-phase with segment gaps in stator, the winding factor has been changed, mainly in coil pitch factor.

The plots of line voltage and spectra have been calculated as shown in Figure 7. For this machine, the rated speed is 12,000 rpm. The magnitude of fundamental back-EMF is 375.8 V.

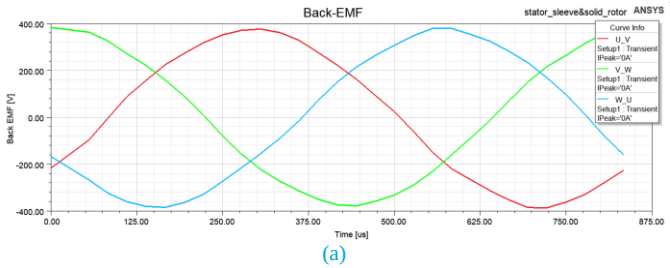

(a)

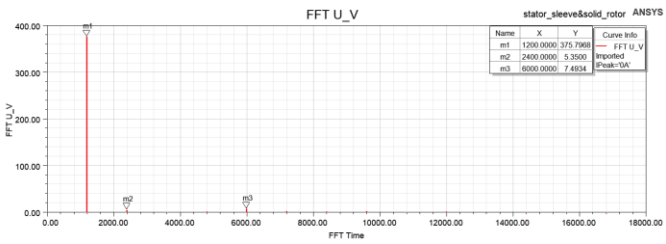

(b)

Figure 7. FEA results of three-phase. (a) single modular back-EMF voltage @ 12,000 rpm. (b) Spectra.

On-load

Torque

At the rated-speed operation, 12000 rpm, the output performance has been checked. The fluctuation of output torque is shown in Figure 8, while the average output torque, ***T****avg*, is 28.3 Nm. Due to the output power meets the requirements. When the machine operated under the healthy operation, the effect of radial force could be negligible. As a fault tolerant application, the triple three-phase machine could maintain operation in the presence of faults, such as the faulty segments will be isolated due to the safety strategy. It is worth to investigate the comparison of radial force under healthy and faulty operations. The rotor radial force under the healthy operation is about13.2 N, as shown in Figure 9.

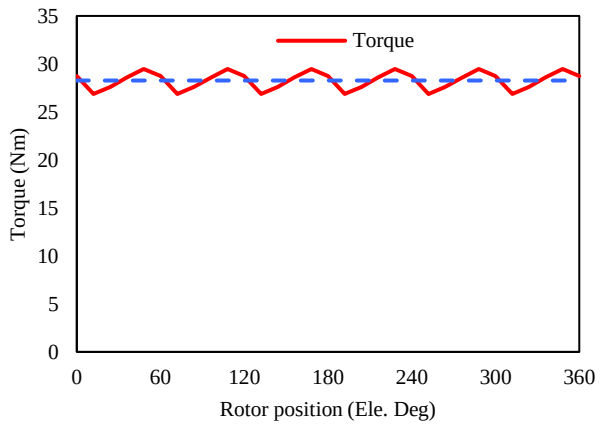

Figure 8. Output torque verse rotor position at 12,000 rpm

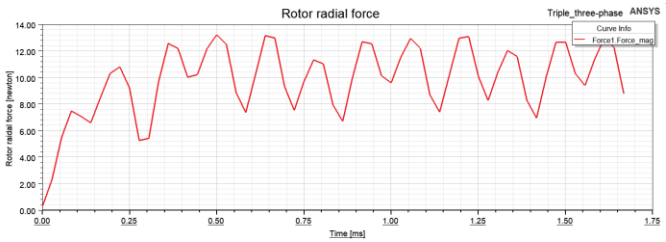

Figure 9. The radial force on rotor under the on-load operation.

Loss

The selection of stator lamination materials, N10 0.1 strip, is able to accommodate the 1200 Hz fundamental frequency and the high core saturation flux density needed to achieve high power density. The rotor magnets array is segmented and laminated in the axial dimension. Moreover, the 3-mm thickness magnet slices could be coated with a thin insulation coating to minimize eddy current loss.

After a short duration, the core losses comprising of eddy current and hysteresis loss are stable as shown in Figure. 10. Besides, the conduction losses in the stator windings are typically the main source of loss in permanent magnet synchronous machines, which are the sum of two components: the Direct Current (DC) loss and the Alternating Current (AC) loss. The DC loss could be predicted easily by theoretical equations, whereas the AC loss is a more complex combination by different effects, skin effect and proximity effect. Based on the different method, the loss distribution of the machine is shown in Table 5.

Meanwhile, the efficiency map from standstill to maximum speed is exhibited which made clear the visualization of values of torque-speed with the efficiency values, in Figure 11.

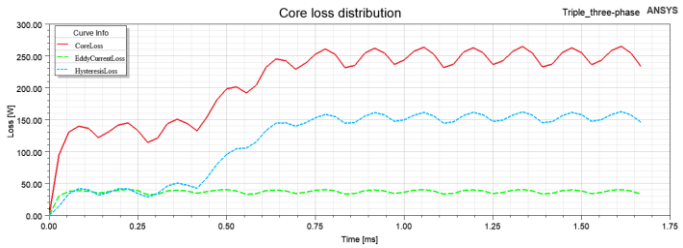

Figure 10. Core loss and its components: eddy current loss and hysteresis loss

Table 5. Loss distribution

Loss	Core loss	Magnet loss	DC loss	AC loss	Total loss
Value (W)	265.0	23	839	324.2	1447

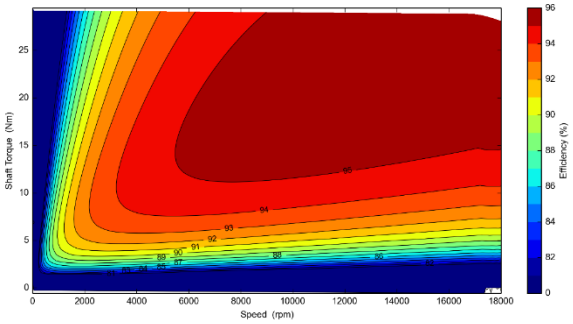

Figure 11. Efficiency map of the whole speed range

Faulty scenarios

As the requirement of fault tolerance for this machine, it should maintain operation continuously in the presence of electrical faults, in other words, short circuit or open circuit faults in the windings. Generally, the potential fault mode could be one single-point fault or combinations. Even there are three three-phases/modules, 9 phases, in this machine, the potential failure modes are limited due to the fault tolerant design. The single layer fractional slot concentrated windings could avoid the faults between modules, or phases.

Therefore, the potential winding faults of this machine could be partial open circuit or short circuit in single module or single phase. The investigate of post-fault performance could pave the way for the corresponding safety strategy. To simplify the investigation, the fault has been supposed in one set of three-phase, Module3 (M3) and others are healthy. The potential failure modes and fault's location are listed in Table 6. Meanwhile, the equivalent circuit diagrams of M3 under varied operations have been illustrated in Figure 12. All of the faulty operations have been simulated respectively.

Table 6 Potential failure modes and fault's location.

Failure mode	**Module status**		
	M1	M2	M3
Partial open-circuit	Healthy	Healthy	Faulty
Partial short-circuit	Healthy	Healthy	Faulty
	Healthy	Healthy	Turn-to-turn faulty

Three-phase (M3) open-circuit

The open-circuit faults have been assumed occurred in the M3, replacing the real resistance by a giant one as shown in Figure 12(b). There is no current flow in the circuit, nor energy conversion. The machine will lose similar ratio output power, according to the absence of phases. Therefore, the degradation of performance is also predictable.

Compared with normal operation, the case of three-phase open-circuit has been examined and compared in Table VII. Because of the absence of one three-phase, output torque has been reduced one third. Torque ripple increases slightly, but maximum radial force spikes dramatically due to the winding arrangement. In short, the machine could be faulty-safe and maintain operation with about two thirds power, with higher torque ripple.

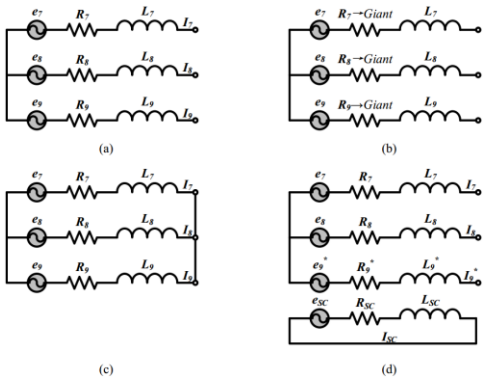

Figure 12. M3 equivalent circuit under varied scenarios (a) Healthy. (b) Open-circuit. (c) Symmetrical short-circuit. (d) Turn-to-turn short-circuit of Phase 9 in M3.

Table 7. Output comparison under varied scenarios

Mode	**Torque (Nm)**	**Torque ripple (%)**	**Max. radial force (N)**
Healthy	28.3	9.2%	13.2
M3 open-circuit	19.0	11.6	171.4

Three-phase (M3) short-circuit

The three-phase short-circuit (SC) could be illustrated by the equivalent circuit as shown in Figure 12(b). This sort of fault is possible to occur by the faults in the power electronics. The behavior and impact of short-circuit are more sophisticated than open-circuit because the SC current is exist continuously in the windings.

The fluctuations of output are shown in Figure 13. The SC current comprising of AC and DC components will restore sinusoidal status after a short duration while the DC attenuation as shown in Figure 13 (a). The drag torque generated by SC current in the phases of M3 will play a role of brake, reluctant effect to the output torque. Meanwhile, the SC operation causes a shock for machine resulting higher torque ripple and rotor radial force.

The fluctuation of metrics in the post-fault operations, between open-circuit and short-circuit, are totally different. In the former scenario, the radial force increases dramatically and maintains, as well as torque ripple. Oppositely, the peak value will adjust from peak value to relative lower value. By selection proper bearing pairs, the faulty machine could operate continuously.

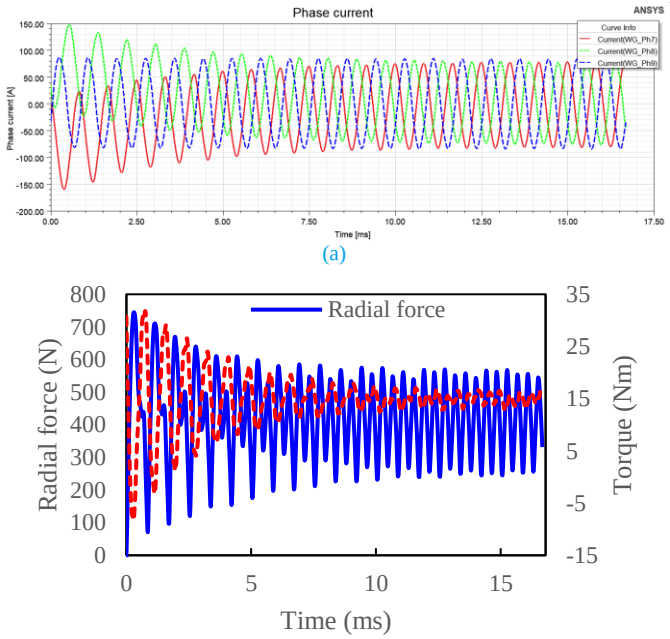

Figure 13. Output of the machine under three-phase short-current. (a) Phase current plots. (b) Fluctuation of radial force and torque.

Turn-to-turn SC

As aforementioned, the most severe fault for electrical machine is the turn-to-turn short-circuit, which caused by the failure of insulation in coil. In this model, a turn-to-turn fault is supposed in Phase 9 (M3). The SC turns and remaining healthy parts of phase 9 are magnetically coupled but electrically isolated, as the equivalent circuit shown in Figure. 12(d). The coil of phase 7 could be split into two independent parts with random turns.s the SC current flow exists in the independent circuit.

The turns of SC winding and its location in the slot are the key variables to affect the SC current [28]. And, the most severe condition is the single-turn SC fault occurs closer to the slot opening, as shown in Figure. 14. The target of this model is to investigate the potential maximum SC current in the coil. To estimate the worst case,

the model of single turn short circuit which close to the slot-opening is proposed as illustrated in Figure. 14.

The output torque under this specific fault is shown in Figure. 15. The output torque 26.3 Nm is slightly lower than healthy output 28.3 Nm. The torque ripple increases dramatically, from 9.2% to 34.2%, which could be a criterion for fault diagnosis to evaluate if turn-to-turn short-circuits is occurring. The main challenge under this fault is the SC current, which is high enough to affect adjacent healthy winding for the thermal concern. The potential safety strategy to cope this sort of fault is to downgrade output by low speed and load.

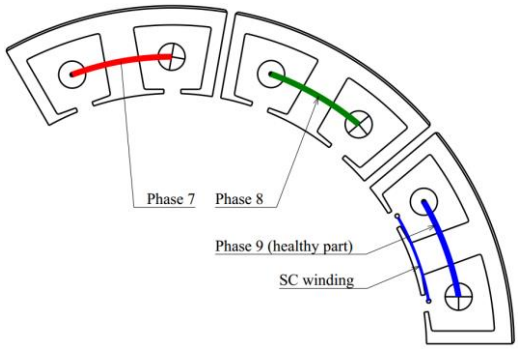

Figure 14. schematic diagram of SC winding and healthy winding of Phase 9 in the module 3 (M3)

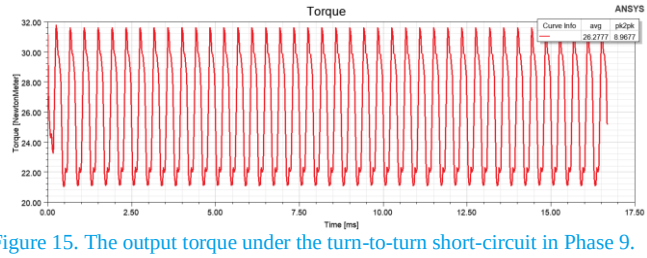

Figure 15. The output torque under the turn-to-turn short-circuit in Phase 9.

Thermal management

As abovementioned introduction, the optimal design could be operated continuously which is supported by proper thermal management. In this case, the current density for continuous operation is 9 A/mm^2.

The thermal management selection for this machine is based on the maximum allowed temperatures. The safety threshold of these temperatures for critical motor components or parts are totally different. To adapt the high temperature risk of operation environment and avoid demagnetization, samarium cobalt (SmCo), Recoma 33E (supplier: Arnold Magnetic Technologies) has been adopted as Permanent magnet. The maximum operating temperature of Recoma 33E is 350 °C, which is much higher than neodymium–iron–boron permanent magnets (NdFeB). Whereas, the safety temperature limitation of windings are 200 °C for the concern of insulation materials. In other words, the selected cooling solution should maintain these components safely during the continuous operation.

The target of feasible cooling method should resolve the heat transfer consisted of conduction and convection of machine components. The main heat source, machine loss, is from winding loss which the quantitative research has been investigated in detail.

Selection of cooling method

The designed modular machine has nine independent stator segments, consisted of coil and stator back iron, which means the potential advantages in interchangeability and serviceability. The faulty segment could be extracted and replaced with a new one easily. So, the potential cooling solution should keep inner space simple and the segments away from coolant. Based on these requirements, the internal cooling methods are not considered. Above all, as a common external cooling method, housing water jacket is selected for this machine, due to the better cooling performance and manufacturing readiness level.

The cooling paths and shape of cooling ducts are varied. The heat transfer capacity does not determined by the topology, but the total cooling surface. In this machine, housing water jacket with axial cooling path is the optimal choice for the readiness level to manufacture. Computational Fluid Dynamics (CFD) method, is adopted to analysis the thermal behavior.

Influence of segment gap

As the main component of machine loss, the potential hot spots locate in the mid-winding and end-winding. Due to presence of segments gaps, the heat transfer in this position has been changed, from conduction to convection. It is worthy to investigate the influence of segment gap to the thermal behavior.

3D Conjugate heat transfer CFD analyses were performed to observe the full temperature distribution and to identify the location of the hot spots within the machine. Given the negligible power loss expected in the rotor, stationary components only were considered in the analyses. A comparative study was made, this included both the non-segmented design, used as reference case, and the segmented machine. Gaps in-between the segments were assumed to be air in one case and aluminum in another case. Figure.16 shows the configurations considered and the corresponding temperature distributions in the middle section, where the highest temperature was recorded.

The existence of segments gaps has no significant effect on the heat transfer directly. The slight temperature rise observed can be addressed to the increased power loss, however this appear to be negligible. Additionally, it can be seen that the use of a high conductive material, in-between the segments, does not lead to a significant benefit in terms of temperature reduction.

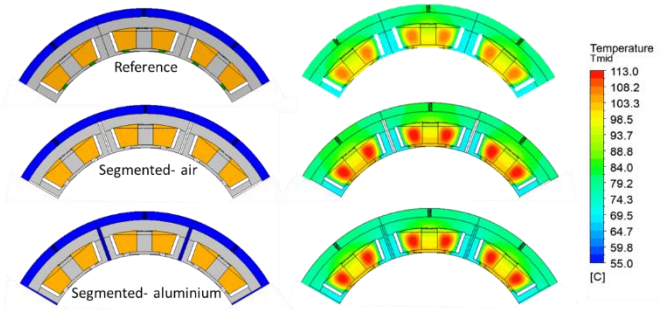

Figure 16. The temperature with varied segment gap size.

Conclusion

A modular triple-three phase has been investigated to meet the specification of starter-generator applied for more electric aircraft. As a safety-critical component to support the electrification of aircraft, the starter-generator candidate should resolve the requirement not only high power density, but also high reliability. The expected candidate could main the operation continuously in the presence of fault. The 18-slot/12-pole triple three-phase topology is a compromise candidate with benefits in cost, redundancy and post-fault performance.

To improve the competence of magnetic isolation, the single layer is selected which exhibits lower mutual inductance. Besides, benefit from the winding arrangement, the whole stator could be split into independent segments which improve fault tolerance further. Meanwhile, the modular design makes the machine interchangeability and serviceability easily.

To investigate the electromagnetic performance thoroughly, a whole model has been created and simulated by finite element analysis method. Besides the healthy operation, the output performance of post-fault have been emulated detailed, such as axial force, torque and torque ripple. As the most severe fault, the turn-to-turn short-circuit has been supposed with extreme assumptions. All the results of post-fault could pave the way for this machine and corresponding control strategy under the faulty scenarios.

Housing water jacket cooling method has been adopted to improve the heat transfer. Although the existence of segment changes the cooling path between segments, the results, which predicted by LPTN, did not exhibit influence. Meanwhile, the temperature distribution proved the machine could continuous operate safely.

In all, this optimal design meet the requirement of this specific application. For the further work, the issue of vibration and noise of this sort of modular stator is worth to investigate. Due to the high speed and high frequency operation, the tangential force of stator segments may be an potential issue. Some material could be chose to fill the gaps, such as the spacer of aluminum, aluminum oxide or steel, to improve the stator sTable. Also, some advanced cooling method could be introduced, such as the winding with potting.

References

1. Wang, B., et al. *Feasibility of Permanent Magnet Fault Tolerant Machines for Aircraft Starter/Generator Systems*. in *2020 International Conference on Electrical Machines (ICEM)*. 2020. IEEE.
2. El-Refaie, A.M., *Fractional-slot concentrated-windings synchronous permanent magnet machines: Opportunities and challenges.* IEEE Transactions on industrial Electronics, 2009. **57**(1): p. 107-121.
3. Dajaku, G. and D. Gerling. *Low costs and high-efficiency electric machines*. in *2012 2nd International Electric Drives Production Conference (EDPC)*. 2012. IEEE.
4. Li, G., et al., *Influence of flux gaps on electromagnetic performance of novel modular PM machines.* IEEE Transactions on Energy Conversion, 2014. **29**(3): p. 716-726.
5. Li, G.-J., et al., *Modular permanent-magnet machines with alternate teeth having tooth tips.* IEEE Transactions on Industrial Electronics, 2015. **62**(10): p. 6120-6130.
6. Zhu, Z., Z. Azar, and G. Ombach, *Influence of additional air gaps between stator segments on cogging torque of permanent-magnet machines having modular stators.* IEEE Transactions on Magnetics, 2011. **48**(6): p. 2049-2055.
7. Heins, G., D.M. Ionel, and M. Thiele, *Winding factors and magnetic fields in permanent-magnet brushless machines with concentrated windings and modular stator cores.* IEEE Transactions on Industry Applications, 2015. **51**(4): p. 2924-2932.
8. Bojoi, R., et al., *Control of shaft-line-embedded multiphase starter/generator for aero-engine.* IEEE Transactions on Industrial Electronics, 2015. **63**(1): p. 641-652.
9. Yaramasu, V., et al., *High-power wind energy conversion systems: State-of-the-art and emerging technologies.* Proceedings of the IEEE, 2015. **103**(5): p. 740-788.
10. Dai, J., et al., *Medium-voltage current-source converter drives for marine propulsion system using a dual-winding synchronous machine.* IEEE Transactions on Industry Applications, 2014. **50**(6): p. 3971-3976.
11. Jiang, X., et al., *Electric drive system of dual-winding fault-tolerant permanent-magnet motor for aerospace applications.* IEEE Transactions on Industrial Electronics, 2015. **62**(12): p. 7322-7330.
12. Sangha, P. and T. Sawata. *Design and test results for dual-lane fault-tolerant PM motor for safety critical aircraft actuator*. in *2015 IEEE Energy Conversion Congress and Exposition (ECCE)*. 2015. IEEE.
13. Valente, G., et al., *Radial force control of multisector permanent-magnet machines for vibration suppression.* IEEE Transactions on Industrial Electronics, 2017. **65**(7): p. 5395-5405.
14. Wang, B., et al., *Optimization and Analysis of a High Power Density and Fault Tolerant Starter–Generator for Aircraft Application.* Energies, 2021. **14**(1): p. 113.
15. Ganev, E., *High-reactance permanent magnet machine for high-performance power generation systems.* SAE Transactions, 2006: p. 888-897.
16. Jiang, X., et al., *Design and optimization of dual-winding fault-tolerant permanent magnet motor.* CES Transactions on Electrical Machines and Systems, 2019. **3**(1): p. 45-53.
17. Arumugam, P., et al., *Analysis of vertical strip wound fault-tolerant permanent magnet synchronous machines.* IEEE Transactions on Industrial Electronics, 2013. **61**(3): p. 1158-1168.
18. Boglietti, A., et al., *Evolution and modern approaches for thermal analysis of electrical machines.* IEEE Transactions on industrial electronics, 2009. **56**(3): p. 871-882.
19. Boglietti, A., A. Cavagnino, and D. Staton, *Determination of critical parameters in electrical machine thermal models.* IEEE transactions on Industry Applications, 2008. **44**(4): p. 1150-1159.
20. Sciascera, C., et al., *Analytical thermal model for fast stator winding temperature prediction.* IEEE Transactions on Industrial Electronics, 2017. **64**(8): p. 6116-6126.
21. Popescu, M., et al., *Thermal analysis of duplex three-phase induction motor under fault operating conditions.* IEEE Transactions on Industry Applications, 2013. **49**(4): p. 1523-1530.
22. Zhang, H., et al., *Comparative study on two modular spoke-type PM machines for in-wheel traction applications.* IEEE Transactions on Energy Conversion, 2019. **34**(4): p. 2137-2147.
23. Zhang, F., et al., *Back-iron extension thermal benefits for electrical machines with concentrated windings.* IEEE

Transactions on Industrial Electronics, 2019. **67**(3): p. 1728-1738.
24. Madonna, V., et al., *Improved thermal management and analysis for stator end-windings of electrical machines.* IEEE Transactions on Industrial Electronics, 2018. **66**(7): p. 5057-5069.
25. Gronwald, P.-O. and T.A. Kern, *Traction motor cooling systems, a literature review and comparative study*. IEEE transactions on transportation electrification, 2021.
26. Ishak, D., Z. Zhu, and D. Howe, *Comparison of PM brushless motors, having either all teeth or alternate teeth wound.* IEEE Transactions on Energy Conversion, 2006. **21**(1): p. 95-103.
27. Barcaro, M., N. Bianchi, and F. Magnussen, *Analysis and tests of a dual three-phase 12-slot 10-pole permanent-magnet motor*. IEEE Transactions on Industry Applications, 2010. **46**(6): p. 2355-2362.
28. Jiang, Y., et al., *Three-phase current injection method for mitigating turn-to-turn short-circuit fault in concentrated-winding permanent magnet aircraft starter generator*. IET Electric Power Applications, 2018. **12**(4): p. 566-574.

Contact Information

Bo Wang
Bo.wang1@nottingham.ac.uk
University of Nottingham
NG8 1BB

Acknowledgments

This project has received funding from the Clean Sky 2 Joint Undertaking under the European Union's Horizon 2020 research and innovation programme under grant agreement No 737814. The author Bo Wang also thanks the studentship from China Scholarship Council.

.